

## Magnetic grating echoes from laser-cooled atoms

A. Kumarakrishnan, S. B. Cahn, U. Shim, and T. Sleator

Department of Physics, New York University, 4 Washington Place, New York, New York 10003

(Received 4 August 1997; revised manuscript received 13 August 1998)

We have used two sets of orthogonally polarized traveling-wave pulses separated in time to establish and, subsequently, rephase a spatially periodic coherence grating between the magnetic sublevels of the  $F=3$  ground state in a cloud of laser-cooled  $^{85}\text{Rb}$  atoms. The rephasing results in a magnetic grating echo (MGE). We have used the shape of the signals to determine both transverse and longitudinal velocity distributions and to study the effects of magnetic fields. The amplitude of the MGE with counterpropagating pulses is modulated at the atomic recoil frequency, a consequence of matter wave interference. [S1050-2947(98)50411-8]

PACS number(s): 03.75.Dg, 06.20.Jr, 32.80.Pj, 42.50.Md

It has been widely appreciated that photon echo techniques may be used for atom interferometry [1,2]. These experiments rely on a sequence of pulses separated in time to create superpositions of atomic states that may subsequently be rephased. Of particular interest are interferometers that involve optically induced coherences between ground states of laser-cooled atoms and afford the possibility of long observation times (the transit time of atoms through the interaction region). A scheme using coherent superpositions of hyperfine ground states has been used for precision measurements of  $\hbar/m$  [3], gravitational acceleration [4], and rotation [5]. Other atom interferometers that employ either microfabricated structures or optical standing waves as beam splitters for atomic beams can be used for a variety of precision measurements in atomic physics as well as for the fabrication of nanostructures and have been reviewed in [6].

In typical echo experiments, the excitation pulses may be traveling waves, as in a two-pulse echo [7], or standing waves, which result in spatially modulated populations (or ‘‘population gratings’’). These population gratings can involve either an excited state [8] or the ground state [9]. Alternatively, the excitation may consist of two simultaneous traveling waves at an arbitrary angle with *orthogonal* polarizations. Such a field configuration produces a spatially periodic *coherence* grating associated with the excited state [10] or the ground state [11–13] (as in this work). All echo experiments have the useful feature that the entire distribution of velocities that are initially excited may subsequently be rephased at the echo points.

Here, we report observations of coherence grating echoes following proposals in Refs. [11,12]. In our experiments, a spatially modulated coherence is created between  $\Delta m = 2, 4, 6$  magnetic sublevels of the  $F=3$  ground state in  $^{85}\text{Rb}$  [Fig. 1(a)] by an excitation pulse consisting of two opposite circularly polarized traveling waves ( $\Delta m \equiv m' - m$  for magnetic quantum numbers  $m'$  and  $m$ ). The pulses have wave vectors  $\mathbf{k}_1$  and  $\mathbf{k}_2$ , which are either at a small angle  $\theta$  (forward) or nearly counterpropagating (backward). The resulting coherence is spatially modulated according to  $\rho_{m,m'}(x,t) = \exp[i(m-m')\Delta\mathbf{k}\cdot\mathbf{x}]\rho_{m,m'}(t)$ , where  $\rho_{m,m'}(x,t)$  is a component of the ground-state density matrix and  $\Delta\mathbf{k} \equiv \mathbf{k}_2 - \mathbf{k}_1$ . We observe this coherence grating by applying a  $\sigma^+$ -polarized ‘‘readout’’ pulse along  $\mathbf{k}_2$ . This field transfers some of the  $\Delta m = 2$  ground-ground coherence into a ground-excited coherence, which, due to phase-matching conditions,

radiates a  $\sigma^-$  field along the direction  $\mathbf{k}_1$ . The radiated field is detected with an optical heterodyne arrangement [Fig. 1(b)], and the resulting signal is referred to as a magnetic grating free-induction decay, or MGFID. Higher-order coherences involving  $\Delta m = 4, 6$  do not produce coherent radiation in response to the readout pulse, and are therefore not observable by this detection technique. Thermal motion will cause the grating to dephase on a time scale of  $2\pi/(\Delta k)(\Delta u_{\Delta k})$  where  $\Delta u_{\Delta k}$  is the rms velocity spread along the direction  $\Delta\mathbf{k}$ . This is the time a typical atom takes to move a distance of a grating spacing  $2\pi/\Delta k$ . Measurement of the dephasing times  $\tau_d = 2\pi/ku\theta$  (forward) and  $\tau_d = 1/ku$  (backward) therefore allows one to determine the most probable speed  $u$  corresponding to the transverse and longitudinal velocity distributions, respectively.

A second excitation pulse with the same field configuration as the first, applied at time  $t=T$  after the first pulse, causes the  $\Delta m = 2$  ground-state coherence grating to rephase and results in a magnetic grating echo (MGE) at times  $t=2T$ . The second excitation pulse will also transform  $\Delta m = 4$  and 6 coherence gratings generated by the first pulse into  $\Delta m = 2$  coherence gratings that rephase at times  $t=3T$  and  $4T$ , respectively. The lifetime of the MGE (the value of  $T$  for which the MGE is half its maximum) is limited only by the transit time through the interaction region and by collisions [13], and for cold atoms can therefore be very large. When the pulse separation  $T$  is large compared to the atomic recoil period  $T_R \equiv (2\pi)2m_{\text{Rb}}/\hbar\Delta k^2$ , the wave nature of the atomic center of mass plays an important role in the resulting

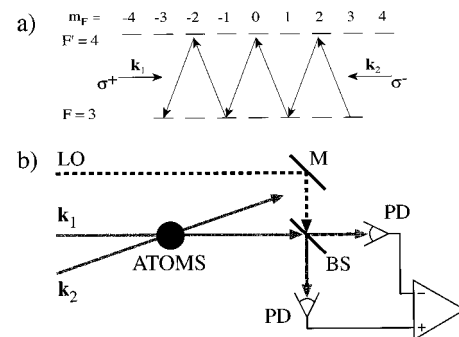


FIG. 1. (a) Level diagram of the Rb transition used in the experiments. (b) Diagram of the experimental configuration: LO, optical local oscillator; M, mirror; BS, beam splitter; PD, photodiode;  $\mathbf{k}_1$  and  $\mathbf{k}_2$  label the excitation beams and readout pulse ( $\mathbf{k}_2$ ).

signal, and the MGE will in general (for  $J \geq 2$ ) show a modulation in  $T$  with period  $T_R$ . This modulation arises from the discrete change of atomic momentum from the photon absorption and emission processes. (In contrast, for  $T \ll T_R$ , as in [8,10,13], the formation of echoes can be explained by an entirely classical treatment of the atomic center-of-mass motion [11].)

In this paper, we present observations of the MGFID and MGE in laser-cooled atoms. We illustrate that the shape of the MGFID and MGE signals is determined by the velocity distribution, and use these signals to infer sub-Doppler temperatures of the atoms in our trap. We also studied the MGFID and MGE signals in the presence of a homogeneous magnetic field, and found that these signals show a modulation that for the “forward” ( $\mathbf{k}_1 \approx \mathbf{k}_2$ ) configuration can be explained by a simple theory involving the effect of rotations on the irreducible components  $\rho_Q^K$  of the atomic density matrix. Finally, we show results for the backward MGE as a function of the time delay  $T$  between excitation pulses, and find the signal to be modulated at the atomic recoil frequency.

In [11], the magnitude of the MGFID and MGE was calculated in the absence of recoil effects under conditions where the excited state could be adiabatically eliminated. The shapes of the MGFID and MGE were calculated to be Gaussians of half width at half maximum  $2/\Delta ku$ . For the cold atoms in our experiments, the most probable speed  $u$  is  $\sim 0.25$  m/s. This ensures that the Doppler width ( $\Delta ku$ ) of the two-photon resonance for both forward ( $\Delta ku \sim 3$  kHz) and backward ( $\Delta ku \sim 0.3$  MHz) excitation is much smaller than the pulse bandwidth ( $\sim 100$  kHz and  $\sim 10$  MHz for the two cases, respectively). Hence, the entire velocity distribution contributes to the signals. It was also pointed out in [11] that when the atom-laser detuning  $\Delta$  is large and spontaneous emission can be neglected, an unequal distribution of populations in the magnetic sublevels of the ground state is necessary to generate the coherence. When the excitation was off-resonance, this was achieved in our experiments by optically pumping the atoms into a specific sublevel. Near resonance, spontaneous and stimulated processes can create sublevel coherences in the absence of additional optical pumping.

A portion of the light from a cw Ti:sapphire laser (linewidth  $\sim 1$  MHz), locked to an external cavity and Rb vapor cell, is split into three sets of retroreflected trapping beams after passing through an acousto-optic modulator (AOM). This AOM frequency shifts the light  $\sim 2\Gamma$  below the  $F=3 \rightarrow F'=4$  resonance in  $^{85}\text{Rb}$  and serves as a shutter for the trap light. A free running diode laser (“repump”) locked to the  $F=2 \rightarrow F'=3$  line optically pumps atoms from the  $F=2$  ground state.

The magneto-optical trap (MOT) [14] is loaded from Rb vapor [15] in a stainless-steel vacuum cell pumped by an ion pump. Three pairs of Helmholtz coils are used to actively cancel the ambient magnetic field during the trapping phase and to apply an arbitrarily directed magnetic field during the experimental pulse sequence. This pulse sequence occurs several milliseconds after the sequential turn-off of the trap light (in  $\sim 100$  ns) and the field gradient (in  $\sim 1$  ms) to allow for the decay of residual eddy currents and for turning on (in  $\sim 2$  ms) the applied magnetic field. Typically, the sample has

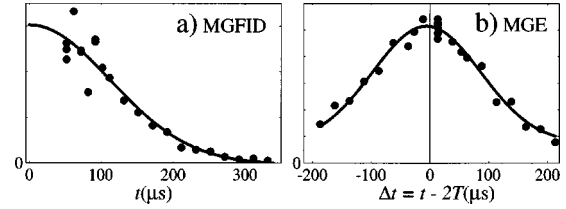


FIG. 2. MGFID and MGE signals obtained by varying the “readout” pulse delay for  $\theta = 9.2$  mrad. Decay time from Gaussian fits:  $158 \mu\text{s}$  in (a), and  $124 \mu\text{s}$  in (b).  $T = 600 \mu\text{s}$  in (b).

a radius of  $\sim 1$  mm during the trapping phase and an optical depth  $\alpha L \sim 1$  (measured by scanning a probe laser across resonance) at the time of the experiment.

Most of the Ti:sapphire light is frequency shifted by a “dual-pass” 80-MHz AOM and split into two beams, each of which passes through a 200-MHz AOM. These AOMs, driven by a common rf oscillator operating at 220 MHz and independently gated by rf switches, produce the orthogonally polarized excitation pulses along directions  $\mathbf{k}_1$  and  $\mathbf{k}_2$ , as well as the readout pulse. The MGFID and MGE signals are observed by applying a readout pulse along  $\mathbf{k}_2$ . The light scattered along  $\mathbf{k}_1$  is combined with the undiffracted cw light (“optical local oscillator” or LO) from the  $\mathbf{k}_1$  AOM on a pair of high-speed Si *p-i-n* photodiodes to produce a 220-MHz heterodyne signal [Fig. 1(b)]. The LO is 220 MHz above resonance, spatially separated from the  $\mathbf{k}_1$  beam, and completely misses the trapped sample. The signal from the photodiodes is mixed with a reference signal from the rf oscillator in a quadrature demodulator. The low-frequency outputs of the demodulator, which represent the real and imaginary parts of the scattered electric-field amplitude, are recorded on a digitizing oscilloscope. If the readout pulse is sufficiently weak, the coherence can be continuously monitored for a few hundred microseconds with minimal perturbation to the atomic system. In cases where the signal is weak, a more intense readout pulse is applied, which destroys the coherence in a few microseconds due to the effects of spontaneous emission. In this case, the onset time of the readout pulse is scanned over the duration of the signal being measured.

Figures 2(a) and 2(b) show the MGFID and MGE (at  $t = 2T$ ) obtained with the excitation pulses applied at an angle  $\theta = 9.2$  mrad. A small quantization magnetic field of  $\sim 0.5$  G was turned on  $\sim 8$  ms after turning off the trap laser and the magnetic-field gradient. Approximately 4 ms later, the atoms were optically pumped into the  $F=3$ ,  $m_F=3$  level by a  $\sigma^+$ -polarized,  $5\text{-}\mu\text{s}$  pulse. Frequency shifts applied to the rf oscillator of the 80-MHz AOM allow the excitation pulses to be detuned  $\sim 60$  MHz above resonance and the readout pulse to be on resonance. This was done to minimize the effect of spontaneous emission during the excitation pulses and maximize the signal. The peak intensities of these pulses correspond to a Rabi frequency  $\Omega \sim 5\Gamma$ . Each data point represents the magnitude of the scattered electric field for a given time delay between the excitation and readout pulses. Gaussian fits to the data of the form  $\exp[-(ku\theta/2)^2 t^2]$  allow us to measure the most probable transverse speed  $u$ .

Since the MGFID lifetime is determined by the most probable speed  $u$ , it can be used to determine the temperature  $\tau$  of the atomic cloud.  $\tau$  corresponds to the velocity distribution probed by the excitation pulses ( $1/e$  radius  $R_p \sim 1.5$  mm) about 12 ms after turning off the trapping beams

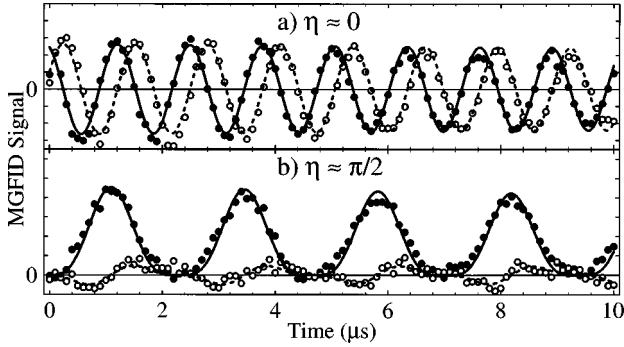


FIG. 3. MGFID signals in the presence of a magnetic field at angle  $\eta$  to the light fields. Points are data (open circles for the imaginary part and closed circles for the real part) and curves are fits of Eq. (1) (the solid curve is the real part; the dashed curve is the imaginary part). (a)  $\eta=0$ ,  $\omega_L/2\pi=390$  kHz. (b)  $\eta=0.47\pi$ ,  $\omega_L=423$  kHz. The duration of the excitation pulse is  $1 \mu\text{s}$ ,  $\Delta=-16.8$  MHz, no optical pumping.

and the field gradient. At these times, the atomic cloud was still smaller than the probe beam, indicating that all atoms in the velocity distribution contributed to the MGFID signal. Measurements of  $\tau$  as a function of the total intensity of the trapping beams (sum of the intensities of all six beams) for intensities in the range from 5 to 65 mW/cm<sup>2</sup> yielded a linear relationship given by  $\tau(\mu\text{K})=28+0.83 I(\text{mW}/\text{cm}^2)$  for a trap laser detuning  $\Delta=-2\Gamma$ . Here, the Doppler limit corresponds to  $\tau=140 \mu\text{K}$ . The sub-Doppler temperatures and the linear dependence of the measured temperature on trap laser intensity are consistent with predictions for the temperature of laser-cooled atoms based on polarization gradient cooling [16]. These results indicate that the MGFID is a simple alternative method for measuring velocity distributions of cold atoms [17–19]. A similar method for measuring the temperature of cold atoms is presented in [20]. We have also used the MGFID to measure the velocity distribution of a room-temperature vapor [13].

When a uniform magnetic field is applied to the atoms, the MGFID shows a modulation at multiples of the Larmor frequency  $\omega_L$  ( $\omega_L$  is the splitting between adjacent  $m$  levels in the presence of a magnetic field). Examples of this modulation are shown in Fig. 3 for two angles  $\eta$  between the magnetic field and  $\mathbf{k}_1$  (nearly parallel to  $\mathbf{k}_2$ ). When  $\eta=0$  [Fig. 3(a)], the signal is seen to be shifted (from dc) to a frequency of  $2\omega_L$ . This can be understood by realizing that the field (which for this case is along the quantization axis) shifts the energies of the magnetic sublevels, resulting in the frequency shift of the signal. That this frequency is at  $2\omega_L$  confirms that the signal is essentially due to the  $\Delta m=2$  coherence between ground-state magnetic sublevels. For  $\eta \neq 0$ , the magnetic field mixes the various  $m$  states, and the modulation is more complex. A simple expression for the signal can be obtained by realizing [11] that the measured signal is proportional to the  $\rho_2^2$  component of the irreducible representation of the atomic density matrix  $\rho_Q^K$ , and that the effect of the magnetic field is to produce a (time-dependent) rotation of the atomic system about the direction of the applied magnetic field. We find that the signal is proportional to the component of the rotation matrix [21] that transforms  $\rho_2^2$  into itself, and is given by

$$S(\eta, t) = [\cos(\omega_L t/2) + i \cos \eta \sin(\omega_L t/2)]^4. \quad (1)$$

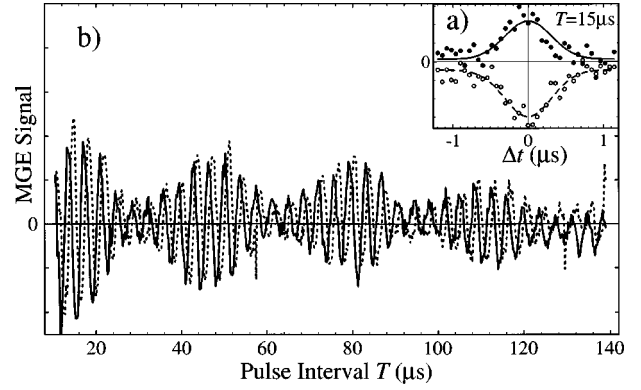


FIG. 4. Backward MGE. (a) Echo signal vs  $\Delta t = t - 2T$  (points) for  $T = 15 \mu\text{s}$ , and fit (curves) of  $\alpha(T)\exp[-(\Delta t/\tau)^2] + \beta(T)$  for complex  $\alpha(T), \beta(T)$ . (b) MGE amplitude  $\alpha(T)$  vs  $T$ . The solid line is the real part of the signal and the dashed line is the imaginary part (no fit shown). The duration of first and second excitation pulses is 0.2 and 0.4  $\mu\text{s}$ , respectively,  $\Delta = -1.9$  MHz, no optical pumping.

Figure 3(b) displays the signal for  $\eta \approx \pi/2$ , which shows a  $\cos^4(\omega_L t)$  dependence, as expected from Eq. (1). Data were taken for several angles, and results were found to be consistent with Eq. (1).

We have also carried out experiments involving two laser fields with orthogonal *linear* polarizations. This field configuration will also produce coherences between ground-state magnetic sublevels, but in contrast to the case of the  $\sigma^+ - \sigma^+$  fields, the coherences will involve (to lowest order) both the components  $\rho_Q^1$  and  $\rho_Q^2$  of the ground-state density matrix  $\rho_Q^K$  [11,22]. In particular, for a quantization axis along one of the directions of linear polarization, the relevant quantities are  $\rho_{\pm 1}^1$  and  $\rho_{\pm 1}^2$ . The different behavior of the  $K=1$  and  $K=2$  components under rotations gives rise to distinct signals in the presence of a magnetic field. We can therefore determine the relative contribution of  $\rho_Q^1$  and  $\rho_Q^2$  by observing the signal in the presence of a uniform magnetic field in various directions.

We now discuss the MGE as a function of pulse interval  $T$ . Measurements of the forward MGE lifetime yielded a value of  $\sim 1.2$  ms for the same conditions as in Fig. 2(b). This is much smaller than the roughly 10-ms time of flight of 200- $\mu\text{K}$  atoms through a probe laser of radius  $\sim 1$  mm. This discrepancy is currently not understood, but could be due to stray light or mirror vibrations. The MGE lifetime in Doppler-broadened vapor, however, has been verified to correspond to the transit time of atoms through the laser beam [13].

We have also measured the MGE for nearly counter-propagating excitation ( $\mathbf{k}_1 \approx -\mathbf{k}_2$ ). Figure 4(a) shows the MGE signal for a pulse interval  $T = 15 \mu\text{s}$ . The signal was detected with a weak readout pulse that was turned on a few microseconds before  $t = 2T$  to record the entire envelope of the echo. The duration of the echo signal (about  $1 \mu\text{s}$ ) is due to the longitudinal velocity spread. Figure 4(b) shows the (complex) amplitude of the MGE as a function of  $T$ , obtained by fitting the echo signal [Fig. 4(a)] to a pair of Gaussian functions. In addition to an overall decay with a lifetime of about 130  $\mu\text{s}$ , the signal possesses a rather complex structure. The oscillation with period 3.65  $\mu\text{s}$  is due to the presence of a magnetic field applied along the direction of the

laser beams, and occurs at a frequency of  $2\omega_L$ . Similar experiments at other magnetic fields support this conclusion. Note that this oscillation does not affect the magnitude of the signal, but represents a  $T$ -dependent phase shift. For the configuration of the experiment, we expect the Larmor phase of the echo signal to cancel at the same times as the Doppler phase, so no Larmor oscillations are expected. We currently have no explanation for this oscillation. The modulation at  $32 \mu\text{s}$  is half the recoil period  $T_R = \pi m_{Rb} / \hbar k^2$ , and is the time for an atom with momentum  $2\hbar k$  (the momentum exchange between atom and fields) to move a grating spacing  $\lambda/2$ . This modulation shows that the quantum-mechanical properties of the atomic center of mass play an important role in this experiment.

For nearly counterpropagating excitation, we were able to measure MGE lifetimes of  $\sim 130 \mu\text{s}$  only in the presence of a uniform magnetic field of  $\sim 0.3 \text{ G}$  or greater along the axis of excitation. The lifetime was smaller for smaller magnetic fields, suggesting the presence of residual field gradients.

From the point of view of the experimental configuration, the work described in this paper is quite similar to that of Ref. [9], in which the cold atomic cloud interacts with an optical standing wave. The physical processes that occur in these two systems, however, are considerably different. In the experiments described in Ref. [9], the two traveling-wave fields making up the standing wave have the same polarization, and the atoms can be modeled in a simple way as two-level systems interacting with a field whose intensity varies periodically in space. The effects observed in that experiment are entirely due to the motion of the atomic center of mass, and atomic recoil plays an essential role. In addition, the signal was found to be insensitive to magnetic fields. In the work described here, the polarizations of the two fields are *orthogonal*, and consequently the light intensity is *uniform* across the sample. The result of the interaction is an

entanglement between the atomic ground-state magnetic sublevels and the atomic center-of-mass motion. The symmetry properties of this superposition of magnetic sublevels can be probed by the effect of a magnetic field on the signal.

Related experiments involving spatially dependent magnetic sublevel coherences have been carried out with an atomic beam [23,24], and recoil effects were also observed. In contrast to the work presented here, Refs. [23,24] made use of dark states to create and detect these atomic sublevel coherences.

In conclusion, we have presented experimental observations in trapped atoms of coherence grating echoes involving superpositions of magnetic sublevels of a single hyperfine ground state [25]. We have shown that measuring the duration of the echo is an accurate and simple method of inferring transverse and longitudinal velocity distributions. This is relevant for understanding the three-dimensional velocity distribution of trapped atoms. As in [9], the MGE as a function of pulse separation was observed to be modulated at the recoil period, indicating the influence of matter-wave interference. Factors limiting the MGE lifetime are not yet understood. We have also studied the influence of magnetic fields on the MGFID and were able to extract information on the symmetry properties of the coherences contributing to the signal. The behavior of MGFID in a magnetic field and the sensitivity of this signal to the atomic velocity distribution suggests the possibility of using magnetic ground-state coherences (in the presence of inhomogeneous magnetic or optical fields) for atomic phase-space imaging [26,27].

We are grateful for helpful discussions with Boris Dubetsky and Paul Berman. We acknowledge financial support from NYU, the U.S. Army Research Office through Grant Nos. DAAH04-93-G0503 and DAAG55-97-1-0113, and the Packard Foundation.

- 
- [1] B. Dubetsky *et al.*, Phys. Rev. A **46**, R2213 (1992).  
 [2] R. Friedberg and S. R. Hartmann, Phys. Rev. A **48**, 1446 (1993).  
 [3] D. S. Weiss *et al.*, Phys. Rev. Lett. **70**, 2706 (1993).  
 [4] M. Kasevich and S. Chu, Phys. Rev. Lett. **67**, 181 (1991).  
 [5] T. L. Gustavson *et al.*, Phys. Rev. Lett. **78**, 2046 (1997).  
 [6] *Atom Interferometry*, edited by P. R. Berman (Academic Press, Cambridge, MA, 1997).  
 [7] I. D. Abella *et al.*, Phys. Rev. **141**, 391 (1965).  
 [8] T. W. Mossberg *et al.*, Phys. Rev. Lett. **43**, 851 (1979).  
 [9] S. B. Cahn *et al.*, Phys. Rev. Lett. **79**, 784 (1997).  
 [10] R. Kachru *et al.*, Opt. Commun. **31**, 223 (1979).  
 [11] B. Dubetsky and P. R. Berman, Laser Phys. **4**, 1017 (1994).  
 [12] B. Dubetsky and P. R. Berman, Appl. Phys. B: Lasers Opt. **59**, 147 (1994).  
 [13] A. Kumarakrishnan *et al.*, **58**, 3868 (1998), demonstrate effects of transit time and collisions on the MGFID and MGE in room-temperature vapors.  
 [14] E. L. Raab *et al.*, Phys. Rev. Lett. **59**, 2631 (1987).  
 [15] C. Monroe *et al.*, Phys. Rev. Lett. **65**, 1571 (1990).  
 [16] J. Dalibard and C. Cohen-Tannoudji, J. Opt. Soc. Am. B **6**, 2023 (1989).  
 [17] D. R. Meacher *et al.*, Phys. Rev. A **50**, R1992 (1994).  
 [18] M. Kozuma *et al.*, Phys. Rev. A **52**, R3421 (1995).  
 [19] C. D. Wallace *et al.*, J. Opt. Soc. Am. B **11**, 703 (1994).  
 [20] Although similar, the work of B. Saubaméa *et al.*, Phys. Rev. Lett. **79**, 3146 (1997), differs from ours in that they create coherences by optically pumping into “noncoupled” states, and employ a different detection technique.  
 [21] B. W. Shore, *The Theory of Coherent Atomic Excitation* (Wiley, New York, 1990), Chap. 18.5.  
 [22] P. R. Berman *et al.*, Phys. Rev. A **48**, 1506 (1993).  
 [23] M. Weitz *et al.*, Phys. Rev. Lett. **77**, 2356 (1996).  
 [24] M. Weitz *et al.*, Europhys. Lett. **37**, 517 (1997).  
 [25] A. Kumarakrishnan *et al.*, in *Quantum Electronics and Laser Science Conference*, 1997 OSA Technical Digest Series Vol. 12 (Optical Society of America, Washington, DC, 1997), p. 117.  
 [26] S. B. Cahn, A. Kumarakrishnan, U. Shim, and T. Sleator, Bull. Am. Phys. Soc. **42**, 1057 (1997).  
 [27] J. E. Thomas (unpublished).